Macroregion size measurements in Bimodal Titanium Forgings using two-dimensional Autocorrelation method

Toubal, Lofti; Bocher, Philippe; Moreau, Andre; Lévesque, Daniel

Publisher's version / la version de l'éditeur:
Metallurgical and Materiels Transactions A, 41, 3, pp. 744-750, 2010-03-01

Web page / page Web
http://dx.doi.org/10.1007/s11661-009-0128-3
http://nparc.cisti-icist.nrc-cnrc.gc.ca/npsi/ctrl?action=rtdoc&an=14607294&lang=en
http://nparc.cisti-icist.nrc-cnrc.gc.ca/npsi/ctrl?action=rtdoc&an=14607294&lang=fr

Macroregion Size Measurements in Bimodal Titanium Forgings Using Two-Dimensional Autocorrelation Method

LOTFI TOUBAL, PHILIPPE BOCHER, ANDRÉ MOREAU, and DANIEL LÉVESQUE

Etching patterns displayed on the surfaces of near-alpha titanium forgings (alloy IMI834) were quantified in terms of sizes and orientations using a two-dimensional (2-D) autocorrelation method. These patterns, which can be associated with local variations of microstructure and further related to regions of specific crystallographic orientations, are known to play a significant role in fatigue and dwell fatigue life predictions. It is then necessary to quantify their dimensions in a manufactured part in order to build a better statistical approach for life prediction in titanium forgings. These distributions of macroregion size and shape were examined on forging cross sections. A data analysis methodology based on a 2-D autocorrelation was used to process sample image data and quantify the macroregion characteristics. The results are more precise than those obtained using a mean linear intercept (MLI) method and additional useful information can be gathered.

DOI: 10.1007/s11661-009-0128-3

I. INTRODUCTION

AN urgent need exists to develop quantitative analysis and methodology for assessing the safety and reliability of titanium alloys in aerospace applications. Unfortunately, the properties in dwell-fatigue of near-alpha alloys vary significantly from one sample to the next.[1,2] A better comprehension of the macrostructures present in the material would enable better engine design and performance.

In fact, local strong texture heterogeneities, called macrozones, are found in forging parts.[1,3–9] These relatively large regions (sometimes having dimensions reaching a few millimeters) present specific crystallographic orientations and play a significant role in the mechanical behavior of parts and their performance. For example, their presence in a highly stressed region of a manufactured part increases dramatically the dispersion in dwell-fatigue life.[8] In this context, only a statistical approach to life prediction could help improve titanium forged part performance.

It is quite difficult to quantify the dimensions of these texture heterogeneities in a manufactured part. Electron backscattered diffraction (EBSD) measurements have been used to image local texture variations.[3–7,9] As such, they allow precise analysis of two-dimensional (2-D) cross sections through the material and through the macroregions. This allows only few macroregions to be imaged at a time. For a statistical estimate of mean dimensions using a large enough number of field of views, the technique would be unacceptably tedious.

However, some local features of the microstructure can be related to the presence of these macroscopic regions and could be used to size these local heterogeneities. In a bimodal near-alpha titanium alloy consisting of a microstructure of 20 pct equiaxed primary α_p grains surrounded by Widmanstätten or columnar secondary α_s grains, the local texture of very large regions was measured by EBSD and revealed that the α_p grains of these macroscopic regions were oriented around a main texture component and, more importantly for the present matter, shared specific sizes and aspect ratios.[6,10] Furthermore, the variations of gray intensities observed on the macroetched surfaces can be related to the presence of macroregions, *i.e.*, various regions sharing primary α_p grains with specific sizes or aspect ratios. These references suggest that it is possible to document the size of the macroregions present in a given region of a forging by estimating the size of the macroetching marks found at the surface of a forging slide.

Practically, macroetching for titanium alloys consists of a few minutes immersion in a 7.5 pct HF, 7.5 pct HNO_3, and 85 pct H_2O solution. The resulting visual aspect in the bimodal near-alpha titanium alloy IMI834 is dull and displays macroetching marks consisting of alternating regions of various gray densities. These gray regions are parallel to the elongation direction of billets and they show the material flow in closed die forged parts, as in Figure 1. Traditionally, this technique is used to evaluate the quality of a forging process; a section of a part is chemically attacked and visually examined.[11] This chemical attack known as macroetching is the most common technique used by process engineers to evaluate the process reliability and the homogeneity of the micro- and macrostructures of

LOTFI TOUBAL, Professor, is with the Department of Mechanical Engineering, Université du Québec à Trois-Rivières, Trois-Rivières, QC G9A 5H7, Canada. Contact e-mail: lotfi.toubal@uqtr.ca PHILIPPE BOCHER, Professor, is with the Department of Mechanical Engineering, École de Technologie Supérieure, Montréal, QC H3C 1K3, Canada. ANDRÉ MOREAU and DANIEL LÉVESQUE, Senior Research Officers, are with the Industrial Materials Institute, National Research Council of Canada, Boucherville, QC J4B 6Y4, Canada.

Manuscript submitted March 20, 2009.
Article published online January 20, 2010

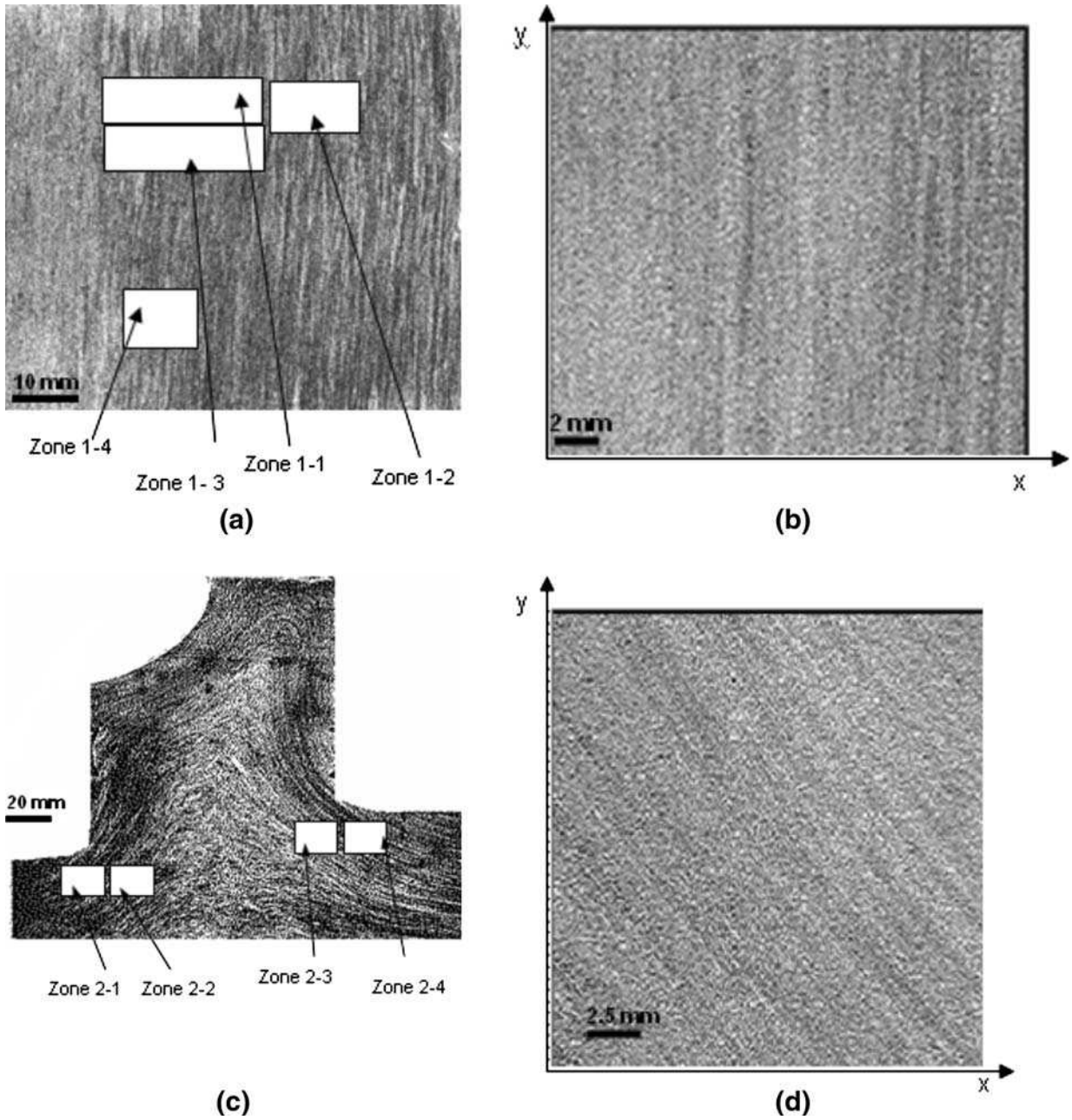

Fig. 1—Optical images of (*a*) billet and the four regions chosen for macroregion size measurements, (*b*) enlargement in zone 1–4, (*c*) forged part showing the four investigated regions, and (*d*) enlargement in zone 2–3.

primary (ingot, bloom, billet, or bar) or secondary (closed die forged part) products. It involves pickling a disc or cross section in strong acid until deep etching displays macroscopic patterns. In this case, macroetching is used to display the so-called ''forging fibers'' or ''flow lines,'' which help gather information on the forging process itself simply by looking at the orientation and direction of the flow lines. This type of inspection is critical for accepting a new forging route and assesses the quality of production batches.

Qualitatively, it is clear that these gray regions have various sizes, shapes, and directions; however, it is quite difficult to give a quantitative estimate of these parameters.[1,3,4] The main objective of this article is to unambiguously estimate the width or spacing between these homogeneous regions. To this effect, we employed two different methods: a modified version of the mean linear intercept (MLI) method[12–20] and an image analysis method based on spatial autocorrelations.[21–25]

II. THE MLI METHOD

One of the most common methods of determining the size of a microstructure is to measure the number of intersections of its boundaries with lines of known

lengths.[12] In the literature, various works using the MLI method to measure the size of grains have been proposed.[12–20] Willis and Lake[13] used the circle intercept method, and they concluded that the use of different measurement techniques in different laboratories results in significant variations in measured grain diameter and grain size distribution. Furthermore, Karlsson and Gokhale[20] proposed a method for estimating the MLI length of anisotropic structures using vertical sections and trisector methods. No measurements of intercept length are required, which makes the method suitable for manual analysis. The purpose of the trisector design is to maximize the precision of the estimator.

The MLI standard method cannot be easily used on macroetched samples because there is no clear feature equivalent to a grain boundary between two macrozones. Instead, there are subtle changes in shades of gray levels. Most likely, it is for that reason that, to our knowledge, optical imaging of macroetched samples has only been used in a qualitative manner.

In the present work, the MLI method was adapted to macrozone imaging. On suitably etched surfaces, macroetched regions are relatively uniform gray levels. The boundary between two regions is a sharp discontinuity between the otherwise uniform gray levels. Imaging or digitizing noise may be superimposed, but if the image is to be useful, this noise either has a small amplitude (a small variation in gray level compared to the variation between two adjacent macrozones) or is uncorrelated over distances much shorter than the macrozone dimensions (usually over distances of order 1 pixel). Let us define a ''macroetched zone'' to be such a surface area of uniform gray level. The macroetched zone could then be the equivalent of a grain in the ASTM E112 standard.[12] For the moment, it does not matter what causes the change in gray level, because, and in practice, we do consider only the changes in gray level. Thus, the present definition of a macroetched zone is a pragmatic one. At the boundary between two macroetched zones, the change in gray level occurs over a much shorter length than the dimensions of the macroetched zone. Thus, the macroetched-zone boundary, *i.e.*, the equivalent of grain boundary in the ASTM E112 standard, is observed as a short-range change in gray level. One of the grain boundary counting methods of the ASTM E112 standard was applied to obtain the macroetched-zone size.

The number of gray level changes in the direction perpendicular to the flow lines was quantified by several people. In the MLI method for the measurement of grain size, the number of grain boundaries is counted and the border between the grain boundaries is often well defined. On the other hand, the borders for titanium macroetched zones are not as well defined and the MLI method is severely limited by the observer's ability to estimate a zone with a uniform gray density.

In our case, each macroregion has a slightly and subtly different shade of gray on a continuous gray scale. Therefore, it is often difficult to determine a border between two macroregions and it is difficult to automate the MLI technique. To determine the reliability of the method, the statistical variability of the measurement was quantified for eight sample regions (four regions on each of two samples) and five different observers. The five observers were selected based on the criteria of being competent and postdoctoral scientists in the measurement sciences. The observers were asked to quantify the number of perceived changes of the gray levels along straight lines perpendicular to the long axis of the macrozones. Each region was marked on the metallic sample. The observers were free to select their own lines near the center of each region. That enabled us to estimate an average value and a standard deviation of the mean measured dimension of macroetched zones. It was found that the macrostructure dimensions are between 0.73 and 0.86 mm in the billet and between 1.00 and 1.09 mm in the forging (Tables I and II). However, the tables reveal that the estimates strongly depend on the observer, by as much as a factor of 3 between the highest and lowest estimates in the billet. Each observer tended to systematically over- or underestimate macroetched zone sizes as compared to the average value for all observers (Section V). This probably indicates that each observer used different criteria to evaluate whether a gray level change occurs. Therefore, the MLI method is strongly subjective and observer dependent.

III. AUTOCORRELATION

Because the determination of a border between two macroregions is often difficult and subjective using the MLI method, an objective mathematical tool is needed to estimate the dimensions of the macroetched zones.

Table I. Widths of the Macroregions (Billet 1) Measured Using the ACF and MLI Methods

Zones	MLI (mm)							ACF (mm) ±0.08
	Obs 1	Obs 2	Obs 3	Obs 4	Obs 5	MLI Average	MLI Standard Deviation	
Zone 1-1	0.96	1.02	0.5	0.73	0.45	0.73	0.26	0.41
Zone 1-2	0.92	1.21	0.86	0.81	0.51	0.86	0.25	0.67
Zone 1-3	0.6	1.66	0.5	0.73	0.32	0.76	0.52	0.33
Zone 1-4	0.62	0.95	0.8	1.00	0.48	0.77	0.22	0.35
Average	0.78	1.21	0.67	0.82	0.44	0.78	—	0.44
Standard deviation	0.19	0.32	0.19	0.13	0.08	0.06	—	0.16

*Obs: Observer.

Table II. Widths of the Macroregions (Forging 2) Measured Using the ACF and MLI Methods

Zones	MLI (mm)							ACF (mm) ±0.08
	Obs 1	Obs 2	Obs 3	Obs 4	Obs 5	MLI Average	MLI Standard Deviation	
Zone 2-1	1.04	1.28	0.83	1.17	0.78	1.02	0.21	0.71
Zone 2-2	0.83	1.66	0.76	1.04	0.70	1.00	0.39	0.67
Zone 2-3	1.04	1.13	1.08	1.34	0.88	1.09	0.17	0.5
Zone 2-4	1.08	1.41	1.08	1.41	0.70	1.08	0.33	0.75
Average	1.00	1.37	0.87	1.24	0.77	1.05	—	0.73
Standard deviation	0.11	0.22	0.14	0.17	0.09	0.05	—	0.14

One such means is the use of autocorrelation functions (ACFs).

Correlation is a mathematical operation used in digital image processing. It consists of measuring the degree of resemblance of two images. When the image is compared to itself, the correlation is called autocorrelation. In this case, two copies of the image are translated with respect to each other. When the two copies are superimposed, the autocorrelation is maximum. When one copy is shifted with respect to the other, the correlation decreases. When the translation is large enough and no similar patterns are found in the image, no correlation can be found and the value of the correlation becomes nearly zero. If repetitive patterns are found in the image, secondary maxima are found on the correlation function and the distance between these maxima is the size of the pattern. The AFC has been used in image analysis to characterize various aspects of the anisotropy of structures. For example, Heilbronner[21,25] used this technique to measure the strain in deformed samples and anisotropy in photomicrographs of geological thin sections. Frykman and Rogon[24] used the ACF to study the image produced from sections through porous media.

To our knowledge, the ACF has been used only twice for characterizing the dimensions of macrozones. The EBSD texture maps were taken on either three perpendicular planes of a sample[4] or on a single plane.[26] The measured orientations and the single-crystal elastic constants were used to calculate the effective elastic constants at all points in the material. Finally, the two-point ACFs of the effective elastic moduli were calculated. The results were used in both cases to calculate the backscattering properties of ultrasound. The ACF was plotted only in the second reference,[26] and macrozone dimensions were not explicitly derived from the calculation.

The mathematical description of the autocorrelation[21,22] can be done by considering $g(x, y)$ the two-dimensional function that defines the image. The 2-D ACF, $G(x, y)$, is defined by the following equation:

$$G(x,y) = \int_{-\infty}^{+\infty} \int_{-\infty}^{+\infty} g(x',y')g(x+x',y+y')dx'dy' \quad [1]$$

where x' and y' are the integration variables. The dimensions of the 2-D autocorrelation are equal to those of the original image. Because the image is of finite dimensions and because it is discretized (*i.e.*, made of pixels), a discrete version (involving summations instead of integrals) of Eq. [1] is used. The discrete ACF can be calculated using fast discrete Fourier transform algorithms, and the correlation in object space can be "reduced" to a multiplication in frequency space.[21,22] It is therefore a straightforward mathematical procedure and numerous software packages exist to perform this operation.

The process used for analyzing the images is summarized in a flow chart in Figure 2. First, samples were machined, polished, and etched with concentrated acid. The second step was the acquisition of images from etched sections in the parts. A regular office scanner (Hewlett-Packard Scanjet, Palo Alto, CA) was used for the acquisition of digital images. These images reflect quite well the differences in gray levels, and they were generally as good as or better than those obtained using a digital camera and various lighting conditions. The images (Figure 1) were recorded in BMP format with 67 pixels per 1-mm length and transformed into text files that could be read with our image processing software. These text files form the basis for analysis and correlation. The third step was the image exploitation and mathematical processing of the selected regions, which is described in Section IV. These regions are selected arbitrarily.

IV. TREATMENT AND PROCESSING

For each sample, regions are selected to measure the width of the macroetched regions. Figures 3 and 4 show the gray scale images of the macrostructures for one region and the related 2-D ACF. In all images, long macrostructures recognized as areas of more or less constant brightness can be observed. It is believed that this brightness depends most strongly on the size and shape of the primary alpha grains and, though indirectly, to the mean crystallographic texture of the macrostructures.[6,9] Therefore, the 2-D ACF provides a quantitative description of the likelihood that gray levels change over all distance scales in the image.

Some large scale variations of brightness do occur in the images. For example, the left side of the billet is, on average, brighter than the rest of the image. Further, the center of the forged part is brighter than the left, top, and right edges. These long-range variations may be caused by a variety of factors (such as uniformity of

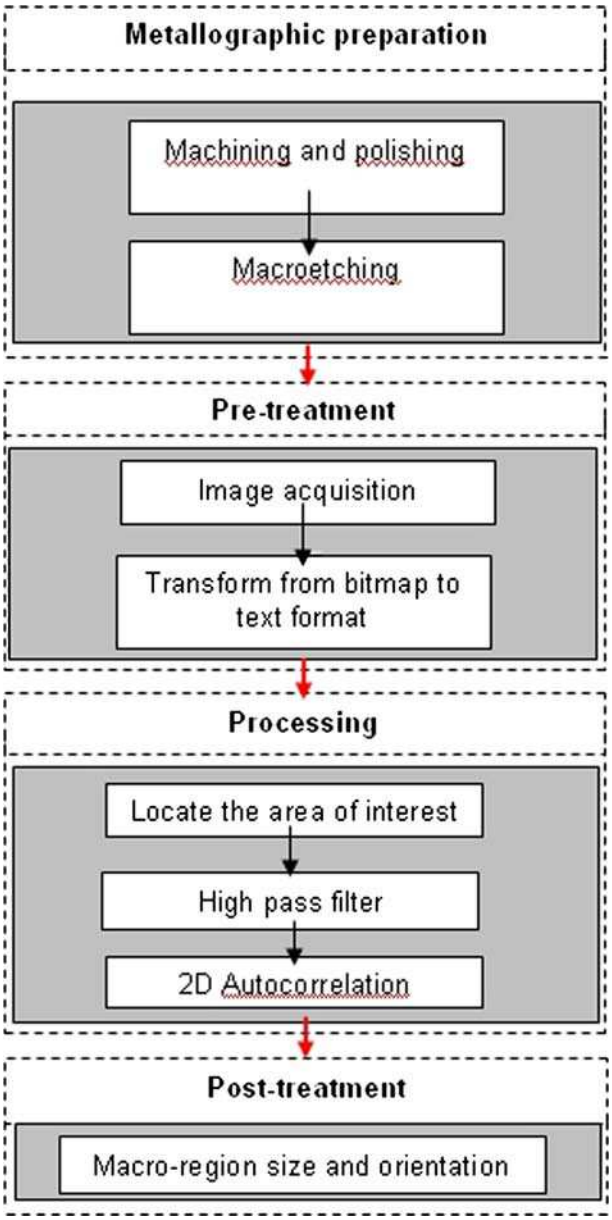

Fig. 2—Flowchart of the procedure adopted for measuring the macroregion size.

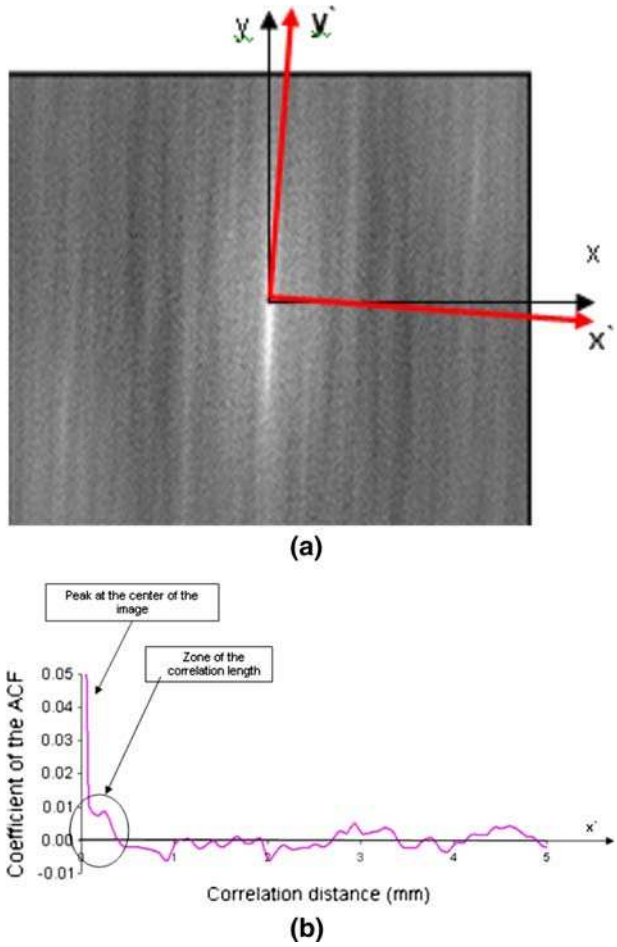

Fig. 3—Representation of the ACF of zone 1–4: (*a*) image in gray scale and (*b*) amplitude profile in (a) along the line perpendicular to the structures.

etch, uniformity of illumination, or others) and are not related to the macrostructures of interest. If these long-range variations are not removed, they will contribute to the ACF. Therefore, they must be removed by applying a 2-D high pass filter to the image before calculating the autocorrelation.

The images of the ACF show the presence of long and tilted structures (Figures 3(a) and 4(a)). The inclination angle of the structures is related to the inclination angle of the macroregions revealed by the chemical attack. The negative values observed on the curves 3b and 4b are the result of the anti-correlation of the values present in the image.[21] The inclination angle and the length of these structures can be estimated from the graph. In this work, we studied the width of the macroregions present in the images.

Figures 3(b) and 4(b) display a bright peak at their left, and Figures 3(a) and 4(a) display a similar peak in their centers. These peaks occur at zero correlation distance, correspond to the maximum of the ACF, and are related to the image contrast and brightness. Generally, the width at half-maximum of this peak corresponds to the average width of the structures present in the image. In our case, the width of this peak (two pixels) is related to the resolution of our images. It is caused by pixel-to-pixel random variations of the gray intensity and is therefore a measurement of image noise. More interestingly, a wider and lower peak is superimposed at the base of this central peak (Figures 3(b) and 4(b)). This secondary peak has a dimension approximately equal to the width of the macroetched zones found in the image by the five independent observers. This peak resembles an exponential decay function with noise superimposed onto it, but other functions could also fit.

To systematically measure the width of this secondary peak, the width at half-maximum is traditionally used, but other criteria can be used as well. For example, if an exponential decay of the signal is expected, the width at 1/e criterion can be used. However, in our work, we had

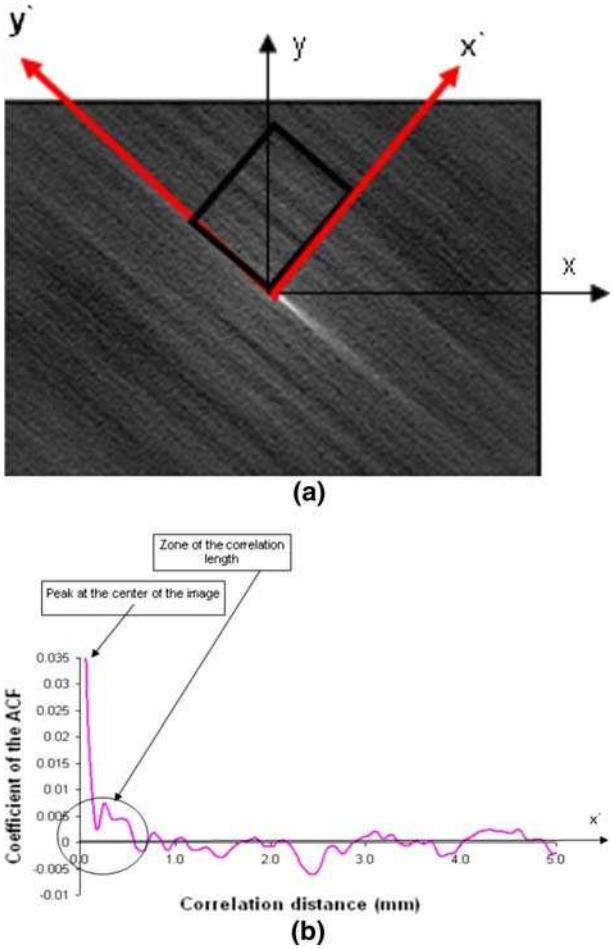

Fig. 4—Representation of the ACF of zone 2–3: (*a*) image in gray scale and (*b*) amplitude profile in (a) along the line perpendicular to the structures.

no reason to assume that the decay would be exponential and the simple criterion of half-width at half-maximum was used. In fact, the criterion to be used is rather subjective, but once selected, it must be kept to avoid biases. Moreover, we expect that the width of the ACF will be a good estimate of the macroregion size, but we also expect that it may differ systematically by a factor of order 1, depending on which criterion is used.

V. RESULTS

The billet is expected to have relatively uniform macrostructures. The average dimension of the macrostructures in the four regions is about 0.78 ± 0.06 mm according to the MLI method and 0.44 ± 0.16 mm according to the ACF method. Therefore, the ACF method gives a value of about 0.56 times that of the MLI method. On the other hand, in the forged sample, the average of all MLI measurements is 1.05 mm and the average of all ACF measurements is 0.73. Thus, we conclude that the ACFs systematically underestimate the dimensions of the macroregions by a factor of about 0.6 to 0.7.

Looking again at the measurements made on the billet sample, we find that the standard deviation of the ACF method, ± 0.16 mm, is comparable to the standard deviation of a single user, between ± 0.08 and ± 0.32 mm, and we conclude that the ACF method and the MLI method are approximately equally precise. We also find that the largest source of variation of the MLI method is due to the observer. It is clear that each observer systematically over- or underestimated the macroregion size as compared to the overall mean, and we must conclude that the MLI method has a very large observer bias.

The ACF method has one significant advantage over the MLI method: it is not affected by observer bias, because the estimate of the peak width is unambiguous. Moreover, the ACF technique can be automated with a suitable numerical implementation inside a computer, while the MLI cannot because of the poor contrast of the images. Those are two reasons why we believe that the ACF is a method that could be used for statistical analysis and process or product validation.

As discussed previously, the ACF method yields smaller values than the MLI method, because it is quite possible that observers cannot distinguish subtle gray variations as well as the ACF can. Moreover, the choice of a criterion for macroregion boundary identification in the MLI method is very subjective and does influence the measurement, whereas only the peak-width measurement method (half-width at half-maximum in our case) has to be specified in the ACF method.

VI. CONCLUSIONS

A method to size the macrostructures revealed by macroetching in titanium forgings (IMI-834) has been proposed in the present article. If the MLI method can quantify microstructure dimensions such as mean grain size, it is difficult to apply for the characterization of macroetched structures because the discrimination criterion is highly subjective and depends on the observer's experience. A new method based on autocorrelation is proposed to circumvent this problem and measure macroetched zone sizes. In contrast to the MLI method, the ACF analysis has two overwhelming advantages: it is independent of observer bias and it can be automated. Moreover, this method gives very interesting information such as the length, the slope, and the periodicity of macrostructures present in the images. The MLI method cannot give this information.

REFERENCES

1. K. Le Biavant, S. Pommier, and C. Prioul: *Fatigue Fract. Eng. M*, 2002, vol. 25, pp. 527–47.
2. L. Toubal, P. Bocher, and A Moreau: *Int. J. Fatigue*, 2009, vol. 31 (3), pp. 601–05.
3. A.P. Woodfield, M.D. Gorman, J.A. Sutliff, and R.R. Corderman: *Proc. 8th World Conf. on Titanium,* Birmingham, United Kingdom, Oct. 22–26, 1995, pp. 1116–23.
4. P.D. Panetta, R.B. Thompson, and F.J. Margetan: in *Review of Progress in Quantitative Nondestructive Evaluation*, D.O. Thompson

and D.E. Chimenti, eds., Plenum Press, New York, NY, 1998, vol. 17, pp. 89–96.
5. F. Bridier, P. Villechaise, and J. Mendez: *Acta Mater.*, 2005, vol. 53 (13), pp. 555–67.
6. L. Germain, N. Gey, M. Humbert, P. Bocher, and M. Jahazi: *Acta Mater.*, 2005, vol. 53 (13), pp. 3535–43.
7. M. Humbert, L. Germain, N. Gey, P. Bocher, and M. Jahazi: *Mater. Sci. Eng. A-Struct.*, 2006, vol. 430 (1–2), pp. 157–64.
8. M.R. Bache: *Int. J. Fatigue*, 2003, vol. 25, pp. 1079–87.
9. L. Germain: Thèse de Doctotat, Université de Metz, Metz, France, 2005.
10. L. Germain, N. Gey, M. Humbert, P. Vo, M. Jahazi, and P. Bocher: *Acta Mater.*, 2008, vol. 56 (16), pp. 4298–4308.
11. *Standard Test Method for Macroetching Metals and Alloys,* ASTM E340-00, ASTM, Philadelphia, PA, 2006.
12. *Standard Test Methods for Determining Average Grain Size,* ASTM E112-96, ASTM, Philadelphia, PA, 2006.
13. D.J. Willis and S.H. Lake: *Scripta Metall. Mater.*, 1987, vol. 21, pp. 1733–36.
14. H. Abrams: *Metallography*, 1971, vol. 4, pp. 59–78.
15. Y. Takayama, N. Furushiro, T. Tozawa, H. Kato, and S. Hori: *Metall. Trans. A,* 1991, vol. 32A, pp. 214–21.
16. K.J. Kurzydlowski and J.J. Bucki: *Scripta Metall. Mater.*, 1992, vol. 27, pp. 117–26.
17. G.F. Vander Voort: *Scripta Metall. Mater.*, 1992, vol. 26, pp. 1785–90.
18. D.J. Willis and S.H. Lake: *Scripta Metall. Mater.*, 1992, vol. 26, pp. 1791–94.
19. L. Ciupinski, B. Ralph, and J. Kurzydlowski: *Mater. Charact.*, 1997, vol. 38, pp. 177–85.
20. L.M. Karlsson and A.M. Gokhale: *J. Microsc.*, 1997, vol. 86 (2), pp. 143–52.
21. R.P. Heilbronner: *Tectonophysics*, 1992, vol. 212 (3–4), pp. 351–70.
22. H.P. William, A.T. Saul, T.V. William, and P.F. Brian: *Numerical Recipes: The Art of Scientific Computing*, Cambridge University Press, Cambridge, United Kingdom, 1986, pp. 381–416.
23. H. Yao, T. Jifeng, and W. Zhonggunang: *Mater. Sci. Eng. A*, 1991, vol. 148, pp. 45–65.
24. P. Frykman and A.T. Rogon: *Comput. Geosci.*, 1993, vol. 19 (7), pp. 887–930.
25. R.P. Heilbronner: *Comput. Geosci.*, 2002, vol. 28, pp. 447–55.
26. M. Humbert, A. Moreau, E. Uta, N. Gey, P. Bocher, and C. Bescond: *Acta Mater.*, 2009, vol. 57 (3), pp. 708–14.